Cite this: DOI: 10.1039/c0xx00000x

www.rsc.org/xxxxxx

ARTICLE TYPE

Mono-and Tetra-nuclear copper complexes bearing bis(imino)phenoxide derived ligands: catalytic evaluation for benzene oxidation and ROP of ε-caprolactone

Xue Wang,[a] Qe-King Zhao,[a] Mark R.J. Elsegood,[b] Timothy J. Prior,[c] Xiaoming Liu,[d] Li Wu,[d] Sergio Sanz,[e] Euan K. Brechin[e] and Carl Redshaw*[a,c]

Received (in XXX, XXX) XthXXXXXXXXX 20XX, Accepted Xth XXXXXXXXX 20XX

DOI: 10.1039/b000000x

Abstract Complexes of the type $[Cu(L)_2]$ (**1**) and $[Cu_4L_2(\mu_4\text{–}O)(OAc)_4]$ (**2**) have been obtained from the reaction of the phenoxydiimine 1,3-(2,6-$R^2{}_2C_6H_3N{=}CH)_2$-5-$R^1C_6H_2OH$-2 (LH) (where R^1 = Me, *t*Bu, Cl; R^2 = Me, *i*Pr) with copper(II) acetate $[Cu(OAc)_2]$; changing the molar ratio of the reactants affords differing amounts of **1** or **2**. Reaction of the parent dialdehyde [1,3-$(CHO)_2$-5-MeC_6H_2OH-2] with $[Cu(OAc)_2]$ in the presence of Et_3N afforded, following work-up, a polymeric chain (**3**) comprising $\{[Cu_2(OAc)_4]OAc\}_n$, $HNEt_3$ and MeCN. The crystal structures of **1** (R^1 = Me, R^2 = *i*Pr **1a**; R^1 = Cl, R^2 = *i*Pr **1b**), **2** (R^1 = Me, R^2 = Me **2a**; R^1 = Me, R^2 = *i*Pr **2b**; R^1 = *t*Bu, R^2 = Me **2c**; R^1 = Cl, R^2 = Me **2d**; R^1 = Cl, R^2 = *i*Pr **2e**; R^1 = *t*Bu, R^2 =*i*Pr **2f**) and **3** are reported (synchrotron radiation was necessary for **3**). The magnetic properties of the cluster **2b** are presented. Complexes of type **2** and **3** were screened for the ring opening polymerization (ROP) of ε-caprolactone, with or without benzyl alcohol present, under a variety of conditions, however only trace polymer was isolated. The electrochemistry of all complexes was also investigated, together with their ability to catalyze benzene oxidation (using hydrogen peroxide); although low conversions were observed, the tetra-nuclear complexes exhibited excellent selectivity.

Introduction

In recent years, ligand frameworks that are capable of binding two transition metals in close proximity have attracted interest, due primarily to the possibilities of beneficial cooperative effects. [1] In the field of lactone polymerization, the coordination/insertion mechanism has drawn analogies with biological systems and in-particular the mechanism of hydrolysis of some metalloenzymes, where one of the metal present can coordinate water thereby lowering its pKa (enhanced nucleophilicity) and generating a hydroxide species. A second metal can then bind the substrate and make it more susceptible to nucleophilic attack. With this in mind, Hillmyer and Tolman probed the potential cooperative influence of the Zn-O-Zn motif in lactide polymerization. [2] We have been interested in the coordination chemistry of acyclic Schiff base ligands and their potential to hold metals in close proximity by utilizing the phenolic group to form an M-O-M linkage. [3] Furthermore, Sun *et al*. reported that cobalt and nickel complexes bearing bis(imino)phenolate type ligands are active for the oligomerization of ethylene. [4] We were also attracted to the potential catalytic ability of copper; complexes bearing *NNO* tridentate Schiff bases have been shown to act as useful catalysts for the copolymerization of carbon dioxide and cyclohexene oxide. [5] In terms of a Cu_4O core, early structural examples utilizing bis(amino)alcohols were reported by Krebbs*et al*, [6] whilst Chaudhuri*et al* have extended such studies to related ONONO-type ligation and have examined the magnetic susceptibility of the resulting Cu_2 and Cu_4 complexes. [7] More recently bis(imino)phenoxy N_2O type ligation has been utilized to isolate complexes that can act as catalysts for the oxidation of cyclohexane and toluene, [8] and in catecholase-like activity. [9] We also note that Pandey *et al* have, by employingβ-ketoaminato ligands, isolated both mono and tetranuclear copper complexes, the formation of which was dictated by the use of anhydrous conditions or not. [10] Herein, we explore the chemistry of the ligand set 1,3-(2,6-$R^2{}_2C_6H_3N{=}CH)_2$-5-$R^1C_6H_2OH$-2 (LH) (where R^1 = Me, *t*Bu, Cl; R^2 = Me, *i*Pr) towards $[Cu(OAc)_2]$ and have structurally characterized both tetranuclear and mononuclear complexes (see scheme1), the yield of each product can be controlled by the reaction stoichiometry. The polymeric product resulting from the interaction of [1,3-$(CHO)_2$-5-MeC_6H_2OH-2] with $[Cu(OAc)_2]$ in the presence of Et_3N is also reported. In terms of catalysis, the tetranuclear complexes and the polymeric complex were screened for their ability to ring open polymerize (ROP) ε-caprolactone, but results were disappointing. We have also investigated the electrochemistry of these complexes and

their ability to catalyze benzene oxidation.

Results and discussion

Synthesis

Bis(imino)phenoxide complexes

Interaction of [2,6-(2,6-*i*Pr$_2$C$_6$H$_3$N=CH)$_2$4-MeC$_6$H$_2$OH] (LH) and [Cu(OAc)$_2$] (two equivalents) in refluxing toluene afforded, following work-up, large green blocks as the major product (*ca.* 90 %) and thin yellow plates as the minor product (*ca.* 10 %), both of which proved to be suitable for single crystal X-ray diffraction.

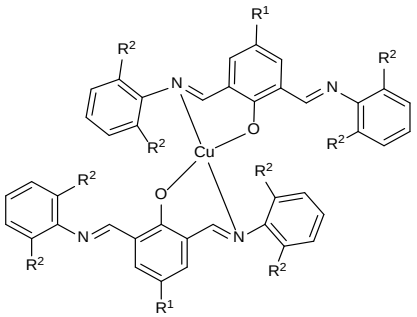

R^1 = Me, R^2 = *i*Pr **1a**
R^1 = Cl; R^2 = *i*Pr **1b**

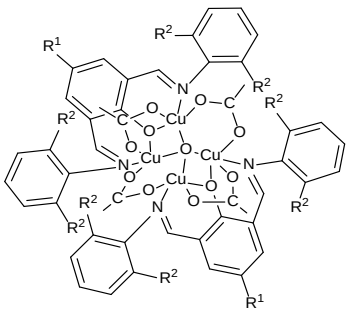

R^1 = R^2 = Me **2a**; R^1 = Me, R^2 = *i*Pr **2b**;
R^1 = *t*Bu, R^2 = Me **2c**; R^1 = Cl, R^2 = Me **2d**;
R^1 = Cl, R^2 = *i*Pr **2e**; R^1 = *t*Bu, R^2 = *i*Pr **2f**

Scheme 1. Copper complexes prepared herein.

The minor yellow complex was shown to be the bis-complex [CuL$_2$] (**1a**), whilst the major green product was found to be the tetranuclear complex [Cu$_4$L$_2$(μ_4–O)(OAc)$_4$] (**2b**). By varying the reaction stoichiometry (L:Cu 1:1 for **1a,b**; 1:2 for **2a-f**, see experimental), it proved possible to also isolate the monomeric complexes **1b** (for R^1 = Cl, R^2 = *i*Pr) and tetrametallic type complexes for R^1 = Me, R^2 = Me **2a**; R^1 = *t*Bu, R^2 = Me **2c**; R^1 = Cl, R^2 = Me **2d,** R^1 = Cl, R^2 = *i*Pr **2e**; R^1 = *t*Bu, R^2 =*i*Pr **2f**.

For the mononuclear complexes, mass spectra exhibited peaks for $[M + H]^+$, whilst in the IR spectra bands at 1612/1617 and 1542 (for type **1** complexes) and 1617 and *ca.* 1550 (for type **2**) cm^{-1} were consistent with the presence of the imine C=N linkage. In the IR spectra of the 'free ligands', two strong absorptions are observed in the region 1580 – 1630 cm^{-1} for the imine stretching mode. There is thus a shift to lower frequency upon coordination. In the case of the phenolic C-O band, there is a shift to higher frequency upon coordination (1327-1347 cm^{-1} in the complexes *versus* 1254 – 1263 cm^{-1} in the 'free ligands').

The IR spectra of the tetranuclear complexes exhibited a number of weak to medium *ν*C-H bands in the 2860 - 3020 cm^{-1} region, together with a weak band at *ca* 566 cm^{-1}, which is known to be associated with the T_2 mode of the Cu$_4$O.[11] In their mass spectra(electrospray), peaks were observed for the fragments resulting from loss of either one or two OAc groups, namely $[Cu_4(OAc)_3(L)_2(\mu_4\text{-}O)]^+$ or $[Cu_4(OAc)_2(L)_2(\mu_4\text{-}O)]^{2+}$. ESR spectra, recorded at ambient temperature and 103 K, exhibited features similar to that reported by Jian *et al* for the complex $[Cu_4OCl_6(C_{14}H_{12}N_2)_4]$ ($g_\perp$ = 2.107, $g_\parallel$ = 2.210); [12] $g_\perp$ values herein were found at about $g_\perp$= 2.42 (see ESI, Figs. S1 – S3).

Solid state structures

General: There are two basic modes of coordination of the ligand observed: (1) bidentate coordination by the ligand through phenoxide and nitrogen; (2) *bis*-bidentate coordination through μ-phenoxide and both imine nitrogen atoms to two copper ions. Bidentate coordination leads to discrete monomeric complexes that feature centrosymmetric binding of the copper ion in a square planar geometry. The *bis*-bidentate arrangement is found in tetrahedral Cu$_4$O clusters that contain a central oxoanion. A third structure type has been observed in the case of [Et$_3$NH][Cu$_2$(OAc)$_4$](OAc)]·MeCN and this does not contain the Schiff base ligand. [Cu$_2$(OAc)$_4$] paddlewheels are linked by bridging bidentate acetate into a 1-D chain.

Monomeric complexes: The compounds **1a** and **1b** display very similar ligands, differing in the replacement of a methyl group by chloride. As has been noted before, the structural demand of a methyl group and chloride are roughly similar and these two compounds are isomorphous, crystallising in the space group $P2_1/c$ with similar unit cell parameters. The complex is centrosymmetric with the 4-coordinate square planar Cu^{2+} ion residing on the inversion centre. For **1a** (collected at 160 K) the Cu–O and Cu–N distances are 1.917(2) and 1.971(2) Å and the N–Cu–O bite angle is 91.73(9) °. For **1b** (collected at 293 K), the analogous values are 1.9129(15) Å, 1.9841(17) Å, and 91.36(7) °. These geometrical parameters are similar to those reported for related [Cu(N–O)$_2$] type systems; Cu–O 1.889(4) [1.880(5)]* – 1.938(5) Å and Cu–N 1.989(7) [1.901(7)]* – 2.021(5) Å. [13] There are no intermolecular contacts of note for either structure. Crystal data for these are contained in Table 2.

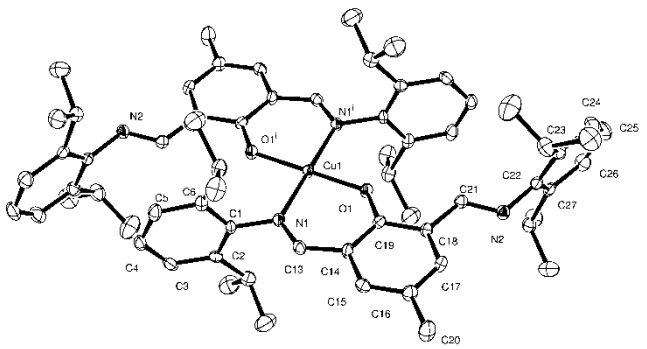

Figure 1.ORTEP representation of the coordination about Cu^{2+} in **1a**, with thermal ellipsoids at 50% probability level. Hydrogen atoms are omitted for clarity. Selected bond lengths (Å) and angles (°): Cu(1) – O(1) 1.917(2), Cu(1) – N(1) 1.971(2), N(1) – C(13) 1.293(4), N(2) – C(22) 1.442(4); O(1) – Cu(1) – N(2) 91.73(9).

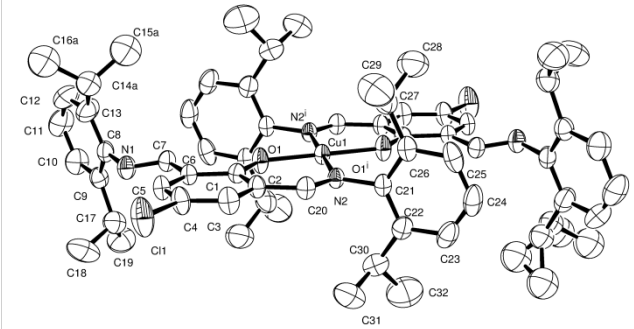

Figure 2. ORTEP representation of the coordination about Cu^{2+} in **1b**, with thermal ellipsoids at 50% probability level. Hydrogen atoms are omitted for clarity. Selected bond lengths (Å) and angles (°): Cu(1) – O(1) 1.9129(15), Cu(1) – N(1) 1.9841(17), N(1) – C(13) 1.282(3), N(2) – C(22) 1.449(3); O(1) – Cu(1) N(2) 91.36(7).

Cu_4O oxo-clusters: Each of the remaining five ligands (L) forms a similar cluster with formula $Cu_4OL_2(OAc)_4$ in which each of the copper ions is five coordinated in a square pyramidal geometry. The cluster contains two ligands, each of which binds two copper ions. The ligands are approximately orthogonal and lie on opposite sides of the cluster. Coordination about the copper is completed by bridging bidentate acetate as shown below. Crystal data for these are contained in Table 3. The central μ_4-oxo is thought to arise due the presence of adventitious oxygen.

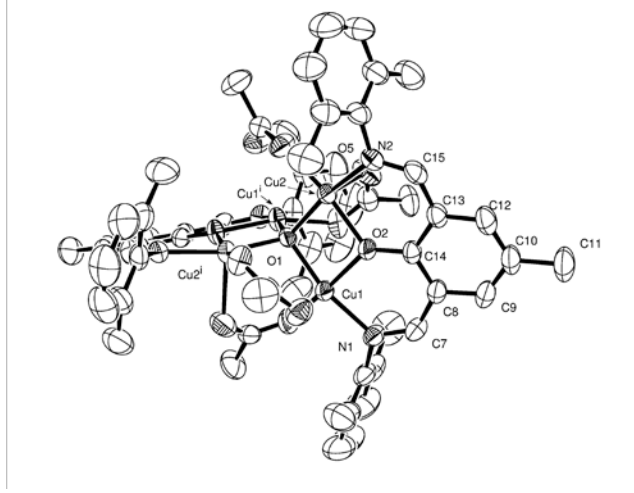

Figure 3. ORTEP representation of the cluster in **2a**, with thermal ellipsoids at 50% probability level. Hydrogen atoms are omitted for clarity. Selected bond lengths (Å) and angles (°): Cu(1) – O(1) 1.9246(17), Cu(1) – O(2) 1.968(3), Cu(1) – O(5) 2.308(4), Cu(1) – O(7) 1.922(4), Cu(1) - N(2) 1.933(4), Cu(1) – Cu(2) 2.9907(10); Cu(1) – O(1) – Cu(2) 79.21(14), Cu(1) – O(2) – C(13) 131.8(2), Cu(1) – O(2) – Cu(2) 79.30(14).

The complex **2c** is representative of the others. Cu–O1 distances within the oxo-cluster lie in the range 1.910(3) to 1.928(3) Å. Coordination by the ligand through O2 and O3 (*i.e.*Cu–O2 and Cu–O3) distances lie in the range 1.968(3) to 1.995(3) Å. Copper-nitrogen distances (ligand) lie in the range 1.988(4) to 2.008(4) Å. Each of these copper ions display square-based pyramidal geometry where the apical Cu–O bond is much longer those bonds in the square plane. For example, for Cu1, Cu–L distances in the plane are 1.928(3), 1.922(4), 1.968(3), 1.993(4) Å, but the apical Cu–O distance is 2.308(4) Å. Each of the structures **2a**, **2b**, **2c**, **2c·MeCN**, **2d, 2e** and **2f** display a very similar cluster and orientation of the pair of ligands. Shown above and below are representations of the cluster in **2a**, **2c** and **2e**.

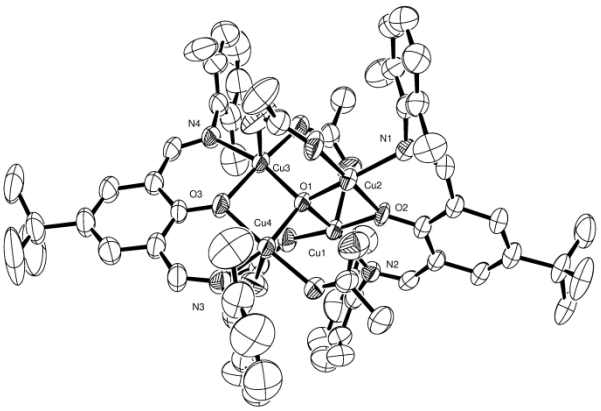

Figure 4. ORTEP representation of the $[Cu_4O]^{6+}$ cluster in **2c**, with thermal ellipsoids at 50% probability level. Hydrogen atoms are omitted for clarity. Selected bond lengths (Å) and angles (°): Cu(1) – O(1) 1.9142(19), Cu(1) – O(2) 1.963(2), Cu(1) – O(6) 1.930(3), Cu(1) – N(1) 1.991(3), Cu(1) – Cu(2) 2.9640(6); Cu(1) – O(1) – Cu(2) 101.15(2), Cu(1) – O(2) – C(14) 131.4(2), Cu(1) – O(2) – Cu(2) 97.22(11).

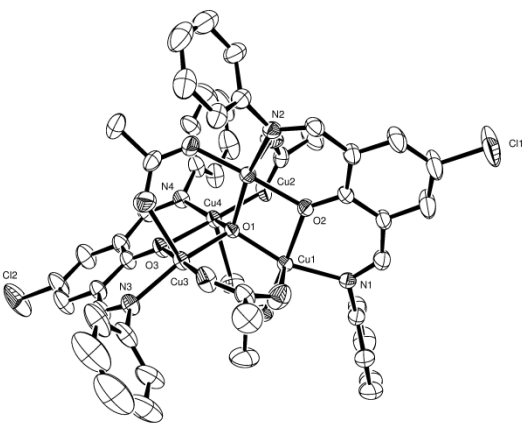

Figure 5. ORTEP representation of the cluster in **2e**, with thermal ellipsoids at 50% probability level. Hydrogen atoms are omitted for clarity. Selected bond lengths (Å) and angles (°): Cu(1) – O(1) 1.914(3), Cu(1) – O(2) 1.992(3), Cu(1) – O(4) 2,235(5), Cu(1) – O(8) 1.908(4), Cu(1) – N(1) 2.014(4); Cu(1) – O(1) – Cu(2) 103.14(14), Cu(1) – O(2) – Cu(2) 98.23(14).

The arrangement of these clusters is unremarkable. There are no hydrogen bonds between the clusters in any case. For some examples, solvent molecules are included in the crystal structure. Full details of stoichiometry and crystal data are found in Table 3.

A search of the Cambridge Crystallographic Database (CSD) for the motif 1,3-$(C(R)N)_2$-C_6H_3O-2 bound to copper found 16 hits for R = Me. Of the non-macrocyclic examples, there was a preference for dinuclear coordination of the bis(imino)phenoxy ligand set as opposed to the mononuclear coordination observed herein for **1a** and **1b**; representative examples are given in reference [14]. We note that 1:1 complexes have been isolated from reactions involving $CuCl_2.H_2O$ and 2,6-bis(imino)phenols. [15] In the case of R = H, there were far more hits (356), of which approximately half (48 %) were macrocyclic, whilst of the remainder, there were 26 hits involving four copper centres bound to a central μ_4-oxo group, 23 of which also involved acetate-type bridging. [7, 8, 14c, 16]

Copper acetate coordination polymer:

Treatment of copper acetate with the dialdehyde 1,3-$(CHO)_2$-5-MeC_6H_2OH-2 in acetonitrile yielded well-formed blue blocks that were found to have the composition $[Et_3NH]^+[Cu_2(OAc)_4(OAc)]^-\cdot CH_3CN$, which contain copper acetate paddlewheels, $[Cu_2(OAc)_4]$, which are linked into undulating 1-D chains by bridging acetate that binds in the terminal site at each end of the paddlewheel. The asymmetric unit is shown below. The bridging acetate assembles the paddlewheels into chains that run parallel to the crystallographic *c* direction (see below).

Between the chains lie Et_3NH^+cations and acetonitrile. The Et_3NH^+cations form a hydrogen bond to acetate through N1. For the hydrogen bond N1–H1···O10, N–H distance = 0.91(2) Å, N···O distance = 2.806(3) Å, N–H···O angle = 172(2) Å. Crystal data for **3** are contained in Table 2.

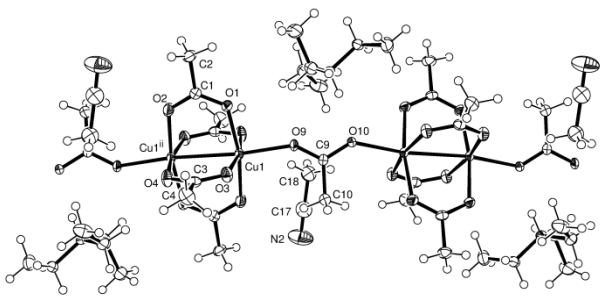

Figure 6. ORTEP representation of a portion of one infinite chain running parallel to *c* in **3**, with thermal ellipsoids at 50% probability level. Selected bond lengths (Å) and angles (°): Cu(1) – O(1) 1.9832(17), Cu(1) – O(3) 1.9648(18), Cu(1) – O(9) 2.1166(15); O(1) – Cu(1) – O(3) 88.72(8).

In the IR spectrum of the polymeric chain $\{[Cu_2(OAc)_4]OAc\}_n$ (**3**), it was not possible to distinguish between the two different types of bridging acetate groups; only a strong broad carbonyl stretch at 1603 cm^{-1} together with a stretch at 1422 cm^{-1} were observable.

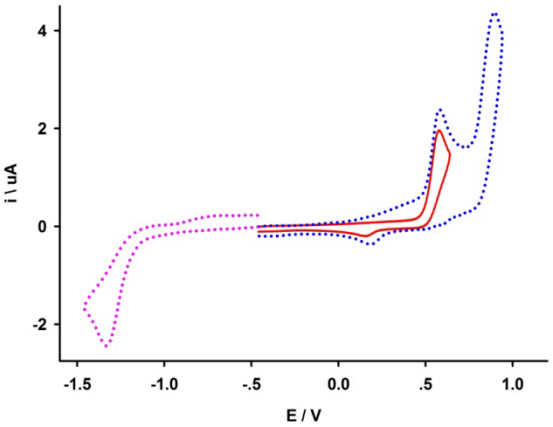

Figure 7. Cyclic voltammograms of complex **1a** (3.2 mmol L^{-1}) in 0.1 mol L^{-1} $[NBut_4]BF_4$–CH_3CN under Ar atmosphere (298 K, scanning rate = 100 mV s^{-1}, red dot-line: reduction process; blue dot- and red solid-lines: oxidation).

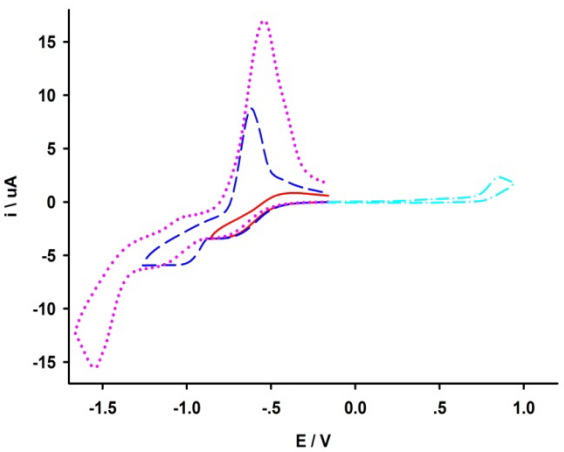

Figure 8. Cyclic voltammograms of complex **2a** (3.2 mmol L^{-1}) in 0.1 mol L^{-1}[N*t*Bu$_4$]BF_4–CH_3CN under Ar atmosphere (298 K, scanning rate = 100 mV s^{-1}, red solid-, blue dash- and purple dot-lines: reduction process; turquoise dot-dash-line: oxidation).

Electrochemistry

The electrochemistry of selected complexes is shown in Figs. 7-9. In the reduction, the first process is attributed to the reduction of Cu(II) to Cu(I) which can be further reduced to Cu(0). The latter reduction is confirmed by the characteristic anodic stripping process, a sharp peak in the returning wave (Figs. 8 and 9). In the cyclic voltammogram of complex **2a**, there are three reduction processes observed between -0.5 and -1.5 V, which is in agreement with its tetra-nuclear core (Fig. 8). For the polymer **3**, further scanning could reveal more reduction processes from Cu(I)

to Cu(0). The reduction potentials of the process, Cu(II)→Cu(I), correlate clearly to the coordinating environment. For the mononuclear complex (**1a**), it possesses two phenolates, whereas the tetra-nuclear cluster (**2a**) possesses on average half a phenolate per metal ion. Due to the strong electron-donating capability of the phenolate, more negative reduction potential is expected for complex **1a** *versus* complex **2a**.

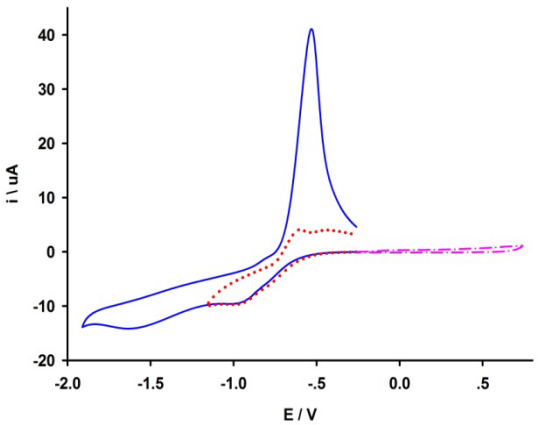

Figure 9. Cyclic voltammograms of complex **3** (3.2 mmol L^{-1}) in 0.1 mol L^{-1} $[NBut_4]BF_4$–CH_3CN under Ar atmosphere (298 K, scanning rate = 100 mV s^{-1} red dot- and blue solid-lines: reduction process; purple dot-dash-line: anodic region).

Magnetic studies

Dc magnetic susceptibility studies on a powdered sample of **2b** (R^1 = Me, R^2 = *i*Pr) were performed in the 300 – 5 K temperature range in an applied field of 0.1 T, and are plotted as the $\chi_M T$ product *versus* T in Figure 7.

The room temperature value of 0.8 $cm^3mol^{-1}K$ is well below that expected for four non-interacting s = ½ ions with g = 2.0 (1.5 cm^3 K mol^{-1}). As the temperature is decreased the value of $\chi_M T$ decreases rapidly to a value of 0.1 cm^3 K mol^{-1} at T = 100 K, before decreasing more slowly to a value of zero at the lowest temperature measured. This behaviour is indicative of the presence of strong antiferromagnetic interactions between the Cu(II) ions. The experimental susceptibility data can be fitted to the simple 2*J* model shown in the inset of Figure 10 and expressed in isotropic spin-Hamiltonian (1) in which J_1 corresponds to the Cu···Cu interaction mediated through one oxo and one carboxylate bridge, and J_2 that mediated *via* one oxo and one alkoxo bridge. The best fit afforded J_1= –192 cm^{-1}, J_2 = –61 cm^{-1} with g = 2.2, values consistent with those previously seen for similar species. [6b, 7, 10] This results in a spin singlet ground state (S= 0) with the first excited (S = 1) triplet state some 384 cm^{-1} higher in energy.

$$\hat{\mathcal{H}}_{ex} = -2J_1(\hat{S}_1\cdot\hat{S}_3 + \hat{S}_1\cdot\hat{S}_4 + \hat{S}_2\cdot\hat{S}_3 + \hat{S}_2\cdot\hat{S}_4) - 2J_2(\hat{S}_1\cdot\hat{S}_2 + \hat{S}_3\cdot\hat{S}_4) \quad (1)$$

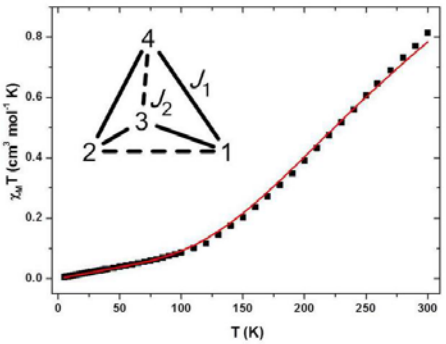

Figure 10. Plot of the $\chi_M T$ product *versus* T for complex **2b** in the T = 300 – 5 K range in an applied field of 0.1 T. The solid red line is a fit of the experimental data to the isotropic model shown schematically in the inset, and spin-Hamiltonian (1).

ε-Caprolactone polymerization

Metal alkoxides are known to initiate the ring opening polymerization (ROP) of lactones. [17] Given this, we attempted to initiate the ROP of ε-caprolactone by addition of benzyl alcohol to the tetranuclear cores, generating metal alkoxides via alkoxy/carboxylate exchange. The complexes were screened in toluene over the temperature range 20 to 120 ^oC and for various ratios of Cu to BnOH over either 12 or 24 h and the results are presented in Table 1. In all cases however, activities were either nil or very low and in the best runs, only trace polymer was isolated. Although the PDI values were low, a plot of M_n *versus* [CL]/[Cu] molar ratio was not linear and so living behavior cannot be inferred. In the MALDI-TOF spectra, only one major population of peaks, which possesses the spacing 114 Da (the molecular weight of the monomer), was detected. The peaks are assigned to the sodium adducts of the polymer chains with benzyloxy end groups. A smaller series of peaks is associated with the use of protonated/sodiated (from the matrix) species. [18] Representative MALDI-TOF spectra are given in the ESI for runs 5 (**2a**) and 7 (**2b**) in Table 1, - see figures S4 and S5. A representative ^1H NMR spectrum (for **2b**, run 7, Table 1) of the PCL is shown in the ESI (Fig. S6), and the peaks in a 5:2 ratio at 7.35 and 5.10 ppm suggested that there was a benzyl ester cap present.

Due to these disappointing results, no further investigation of the potential of these complexes for ring opening polymerization was conducted.

Benzene oxidation

All the complexes catalyzed the direct oxidation of benzene by hydrogen peroxide. Although the mononuclear complex **1a** showed comparable conversion to that we reported recently, its selectivity was rather poor due to over-oxidation of the product phenol. [19] Previously, we observed that in the oxidation of benzene catalysed by copper (II) complexes, the more negative the reduction potential, the higher the conversion of benzene. As

shown in Table 2, the copper (II) clusters exhibited more positive reduction potentials, which may explain their low conversion. What is surprising is that they showed much improved selectivity compared to the monocopper (II) complex. For the clusters, **2c** and **2e**, the selectivity is almost quantitative. The exact reason for this drastic improvement in selectivity is not understood at this stage.

Table 1. ROP of ε-caprolactone using compounds of type **2**[†]

Run	Pre- Cat	T (°C)	CL : BnOH	Time (h)	Conv[a] (%)	$M_{n,GPC}$[b]	$M_{n,Cal}$[c]	PDI
1	**2a**	40	250 : 1	24	--	--	--	--
2	**2a**	60	250 : 1	24	--	--	--	--
3	**2a**	80	250 : 1	24	--	--	--	--
4	**2a**	100	250 : 1	24	3	--	--	--
5	**2a**	110	250 : 1	24	3	374	885	1.01
6	**2a**	120	250: 1	12	10	--	--	--
7	**2b**	100	800 : 1	12	2.2	389	2006	1.01
8	**2b**	120	250 : 1	24	25	2936	7125	1.08
9	**2c**	110	250 : 1	24	22	1644	6270	1.10
10	**2c**	120	250 : 1	12	--	--	--	--
11	**2d**	20	250 : 1	24	20	676	5700	1.02
12	**2e**	110	250 : 1	24	3.5	412	998	1.01
13	**2f**	80	250 : 1	24	--	--	--	--
14	**2f**	100	250 : 1	12	--	--	--	--
15	**2f**	120	400 : 1	12	--	--	--	--
16	**2f**	120	600 : 1	12	--	--	--	--
17	**2f**	120	800 : 1	12	--	--	--	--
18	**2f**	120	1000 : 1	12	--	--	--	--
19	**3**	25	250 : 1	24	--	--	--	--
20	**3**							

[†]Runs conducted in toluene using 0.04 mmol of catalyst; CL = ε-caprolactone.

[a] Determined by ^{1}H NMR spectroscopy,[b] GPC data in THF *versus* polystyrene standard using a correction factor of 0.56 [c] Calculated from $([CL]_0/[BnOH]_0)$ x conv.(%) x Monomer molecular weight.

Table 2. Catalysis of the complexes on direct oxidation of benzene into phenol.[a]

Sample	Conversion (%)	Yield (%)	Selectivity (%)	Reduction potential E_p (V)
1a	31.5	12.2	39	–1.32
2a	7.2	5.5	76	–0.719, –1.019, –1.535
2b	7.6	5.7	75	
2c	7.3	7.6	> 99	
2d	6.9	3.9	57	
2e	7.7	8.7	> 99	
2f	13.4	11.3	84	
3	8.5	7.0	82	–0.963, –1.598

[a] The substrate (benzene) is 10 mmol; the copper complex (0.02 mmol); conducted in 2.5 ml MeCN.

Conclusion

In conclusion, both mononuclear and tetranuclear complexes are accessible form the reaction of 2,6-(2,6-*i*Pr$_2$C$_6$H$_3$N=CH)$_2$-4-MeC$_6$H$_2$OH] (LH) and [Cu(OAc)$_2$], the yields of which can be controlled by variation of the reaction stoichiometry. Changing the substituents at the *ortho* position of the aryl (imino) ring leads to slight variations in the tetrametallic core. The tetrametallic complexes were found to be virtually inactive for the ring opening polymerization of ε-caprolactone in the presence of benzyl alcohol. Magnetic susceptibility studies on the tetrametallic complex with R^1 = Me and R^2 = *i*Pr indicated the presence of strong antiferromagnetic interactions between the Cu(II) ions. The complexes catalyze the hydroxylation of benzene into phenol by hydrogen peroxide. The yields were not superior to others recently reported, however the tetra-nuclear complexes exhibited excellent (near quantitative) selectivities.

Experimental

General

All manipulations were carried out under an atmosphere of dry nitrogen using conventional Schlenk and cannula techniques or in a conventional nitrogen-filled glove box. Diethyl ether and tetrahydrofuran were refluxed over sodium and benzophenone. Toluene was refluxed over sodium. Dichloromethane and acetonitrile were refluxed over calcium hydride. All solvents were distilled and degassed prior to use. IR spectra (nujol mulls, KBr or NaCl windows) were recorded on a Nicolet Avatar 360 FT IR spectrometer; Elemental analyses were performed by the elemental analysis service at Sichuan Normal University. Ligands of type LH were prepared as described in the literature. [7] All other chemicals were purchased from commercial sources and were used as received.

Synthesis of[1,3-(2,6-*i*$Pr_2C_6H_3N{=}CH)_2$-5-MeC_6H_2O-2)]$_2$Cu(**1a**)

2,6-Diformyl-4-methyl-phenoxy(2,6-diisopropylaniline) (0.49 g, 1.0 mmol) and copper diacetate (0.18g, 1.0 mmol) in toluene (30 ml) were refluxed under an argon atmosphere for 12 h. The solvent was then removed *in-vacuo* and the residue was extracted into either hot acetonitrile (25 ml) or ethanol (25 ml). Prolonged standing at ambient temperature afforded **1a** as green/yellow crystals. Yield: 0.18 g, 35 %; elemental analysis calculated for $C_{66}H_{82}CuN_4O_2$: C, 77.19; H, 8.05; N, 5.46. Found: C, 76.68; H,8.15; N, 5.22 %. IR (nujol null, KBr): 3059(w), 3005(w), 2959(s), 2926(s), 2867(s), 2357(w), 1923(w), 1617)s), 1601(w), 1587(w), 1542(s), 1443(s), 1381(s), 1364(s), 1342(m), 1326(m), 1294(m), 1258(s), 1228(s), 1180(s), 1165(m), 1108(w), 1097(w), 1043(w), 978(w), 934(w), 820(m), 798(m), 775(s), 761(w), 702(w), 638(w), 561(w), 520(s), 474(w); MS (ESI): $^m/_z$ 1026 M^+.

Synthesis of[1,3-(2,6-*i*$Pr_2C_6H_3N{=}CH)_2$-5-ClC_6H_2O-2)]$_2$Cu(**1b**)

As for **1a**, but using 2,6-diformyl-4-chloro-phenoxy(2,6-diisopropylaniline) (0.51g, 1.0 mmol) and copper diacetate (0.18 g, 1.0 mmol) affording **1b** as green/yellow crystals. Yield: 0.22 g, 41 %. elemental analysis calculated for $C_{64}H_{76}Cl_2CuN_4O_2$: C, 71.99; H, 7.17; N, 5.25. Found: C, 72.16; H, 7.32; N, 5.13 %.IR (nujol null, KBr): 3066(s), 2961(s), 2095(s), 2866(m), 2356(w), 1737(w), 1612(s), 1588(w), 1542(s), 1436(s), 1385(m), 1367(s), 1332(s), 1292(w),1256(m), 1215(s), 1172(s), 1097(m), 1059(w), 1044(w), 1023(s), 932(s), 871(w), 862(w), 797(s), 771(m), 756(s), 728(s), 697(w), 660(w), 638(w), 562(w), 533(m), 510(m), 481(w). MS (ESI): $^m/_z$ 1068 $[M + H]^+$.

Synthesis of {$Cu_4(OAc)_4$[1,3-(2,6-$Me_2C_6H_3N{=}CH)_2$-5-MeC_6H_2O-2]$_2$(μ_4-O)} (**2a**)

A toluene solution (30ml) of 2,6-diformyl-4-methyl-phenoxy(2,6-dimethylaniline) (0.37g, 1.0mmol), copper diacetate (0.37 g, 2.0 mmol) was refluxed under an argon atmosphere for 12 h. The solvent was then removed *in-vacuo* and the residue extracted in hot acetonitrile (30 ml) or ethanol (30 ml). Prolonged standing (2 – 3 days) afforded **2a** as green crystals. Yield: 0.36 g, 57 %; elemental analysis calculated for $C_{58}H_{62}Cu_4N_4O_{11}$: C, 55.94; H, 5.02; N, 4.50. Found: C, 55.63; H, 5.25; N, 4.31 %. IR (nujol null, KBr): 3447(s), 2924(m), 2856(w), 2362(s), 2337(s), 1612(s), 1549(m), 1452(m), 1394(s), 1341(w), 1262(w), 1181(m), 1074(s), 830(w), 769(w), 719(w), 669(w), 566(w), 517(w), 489(w).MS (ESI): $^m/_z$ 1312 $\{Cu_4(OAc)_2$[1,3-(2,6-$Me_2C_6H_3N{=}CH)_2$-5-MeC_6H_2O-2]$_2$(μ_4-O)$\}^{2+}$

Synthesis of{$Cu_4(OAc)_4$[1,3-(2,6-*i*$Pr_2C_6H_3N{=}CH)_2$-5-MeC_6H_2O-2]$_2$(μ_4-O)} (**2b**)

As for **2a**, but using 2,6-diformyl-4-methyl-phenoxy(2,6-diisopropylaniline) (0.49 g, 1.0 mmol) and copper diacetate (0.37 g, 2.0 mmol) afforded **2b** as green crystals. Yield: 0.44 g, 60 %; elemental analysis calculated for $C_{74}H_{94}Cu_4N_4O_{11}$: C, 60.47; H, 6.45; N, 3.81. Found: C, 60.53; H, 6.93; N, 4.01 %. IR (nujol null,KBr): 3064(w), 2962(s), 2925(s), 2867(s), 2357(w), 1923(w), 1784(w), 1612(s), 1587(s), 1550(s), 1456(s), 1450(m), 1397(s), 1327(s), 1258(m), 1232(w), 1174(s), 1104(m), 1070(s), 1014(m), 932(w), 867(w), 828(w), 800(s), 770(m), 727(m), 665(m), 620(m), 564(m), 528(m), 487(s), 425(w). MS (ESI): $^m/_z$ 1408 $\{Cu_4(OAc)_3$[1,3-(2,6-*i*$Pr_2C_6H_3N{=}CH)_2$-5-MeC_6H_2O-2)]$_2$(μ_4-O)$\}^+$.

Synthesis of {$Cu_4(OAc)_4$[1,3-(2,6-$Me_2C_6H_3N{=}CH)_2$-5-*t*BuC_6H_2O-2]$_2$(μ_4-O)} (**2c**)

As for **2a**, but using 2,6-diformyl-4-*t*-butyl-phenoxy(2,6-dimethylaniline) (0.42 g, 1.0 mmol) and copper diacetate (0.37 g, 2.0 mmol) affording **2c** as green crystals. Crystals suitable for single crystal X-ray diffraction can be grown from either methanol or acetonitrile. Yield: 0.32 g, 48 %; elemental analysis calculated for $C_{64}H_{74}Cu_4N_4O_{11}$: C, 57.82; H, 5.61; N, 4.21. Found: C, 57.71; H, 5.69; N, 4.14 %. IR (nujol null, KBr): 3422(s), 3020(w), 2962(s), 2924(s), 2869(w), 2361(w), 1611(s), 1548(m), 1471(m), 1451(m), 1397(s), 1347(m), 1294(w), 1232(m), 1183(s), 1092(w), 1068(s), 1023(w), 923(w), 891(w), 868(w), 841(w), 797(w), 768(s), 722(w), 667(m), 630(m), 566(m), 510(m), 438(m). MS (ESI): $^m/_z$ 1247 $\{Cu_4(OAc)_2$[1,3-(2,6-$Me_2C_6H_3N{=}CH)_2$-5-*t*BuC_6H_2O-2]$_2$(μ_4-O)$\}^{2+}$.

Synthesis of {$Cu_4(OAc)_4$[1,3-(2,6-$Me_2C_6H_3N{=}CH)_2$-5-ClC_6H_2O-2]$_2$(μ_4-O)} (**2d**)

As for **2a**, but using 2,6-diformyl-4-chloride-phenoxy(2,6-dimethylaniline) (0.39g, 1.0 mmol) and copper diacetate (0.37 g, 2.0 mmol) affording **2d** as green crystals. Yield: 0.37 g, 58 %; elemental analysis calculated for $C_{56}H_{56}Cl_2Cu_4N_4O_{11}$: C, 52.30; H, 4.39; N, 4.36. Found: C, 52.64; H, 4.51; N, 4.53 %. IR (nujol null, KBr): 3437(s), 2973(w), 2918(w), 1612(s), 1546(m), 1471(w), 1440(m), 1395(s), 1342(m), 1316(w), 1258(w), 1226(m), 1179(m), 1092(w), 1059(s), 984(w), 924(w), 883(w), 808(m), 766(w), 720(w), 668(m), 627(m), 565(w), 515(w), 438(w). MS (ESI): $^m/_z$ 1227 $\{Cu_4(OAc)_3$[1,3-(2,6-$Me_2C_6H_3N{=}CH)_2$-5-ClC_6H_2O-2]$_2$(μ_4-O)$\}^{2+}$.

Synthesis of {$Cu_4(OAc)_4$[1,3-(2,6-*i*$Pr_2C_6H_3N{=}CH)_2$-5-ClC_6H_2O-2]$_2$(μ_4-O)} (**2e**)

As for **2a**, but using 2,6-diformyl-4-chloro-phenoxy(2,6-diisopropylaniline) (0.51 g, 1.0 mmol) and copper diacetate (0.37 g, 2.0 mmol) affording **2e** as green crystals. Yield: 0.35 g, 46 %; elemental analysis calculated for $C_{72}H_{88}Cl_2Cu_4N_4O_{11}$: C, 57.25; H, 5.87; N, 3.71. Found: C, 57.36; H, 6.02; N, 3.88 %. IR (nujol null, KBr): 3065(w), 2962(s), 2927(s), 2868(s), 2360(w), 1931(w), 1860(w), 1777(w), 1613(s), 1587(s), 1548(s), 1440(s), 1398(s), 1347(s), 1256(w), 1221(w), 1172(s), 1107(m), 1058(s), 990(w), 932(w), 882(w), 863(w), 791(s), 768(w), 724(s), 667(m), 621(s), 563(m). MS (ESI): $^m/_z$ 991.5 (M^+– L – O).

Synthesis of {$Cu_4(OAc)_4$[1,3-(2,6-*i*$Pr_2C_6H_3N{=}CH)_2$-5-*t*BuC_6H_2O-2]$_2(\mu_4\text{-}O)$} (**2f**)

As for **2a**, but using 2,6-diformyl-4-*t*-butyl-phenoxy(2,6-diisopropylaniline) (0.52 g, 1.0 mmol) and copper diacetate (0.37 g, 2.0 mmol) affording **2f** as green crystals. Yield: 0.52 g, 67 %; elemental analysis calculated for $C_{80}H_{106}Cu_4N_4O_{11}$: C, 61.83; H, 6.88; N, 3.61. Found:C, 61.47; H, 6.96; N, 3.55 %. IR (nujol null, KBr): 3447(s), 2962(s), 2869(w), 1612(s), 1553(m), 1458(s), 1397(s), 1360(w), 1331(w), 1261(s), 1175(w), 1097(s), 1068(s), 1023(s), 931(w), 865(w), 804(s), 725(w), 666(w),623(w), 566(w), 530(w); MS (ESI): $^m/_z$ 1485 {$Cu_4(OAc)_3$[1,3-(2,6-*i*$Pr_2C_6H_3N{=}CH)_2$-5-*t*BuC_6H_2O-2)]$_2(\mu_4\text{-}O)$}$^+$

Synthesis of {[$Cu_2(OAc)_4$](OAc)($HNEt_3$)(MeCN)}$_n$(**3**)

To 2-hydroxy-5-methyl-isophthaldehyde(0.16 g,1.0 mmol) and copper diacetate (0.37 g, 2.0 mmol) was added toluene (30 ml), and the system was stirred at room temperature for 30 min. Triethylamine (0.31 ml, 2.2 mmol) was then added and the solution brought to reflux for 12 h. The solvent was then removed *in-vacuo* and the residue extracted in hot acetonitrile (30 ml). Prolonged standing at ambient temperature afforded **3** as green/blue crystals. Yield: 0.56 g, 66 %; elemental analysis calculated for $C_{18}H_{34}Cu_2N_2O_{10}$ – MeCN (sample dried *in-vacuo* for 2 h): C, 36.64; H, 5.96; N, 2.69. Found: C, 36.83; H, 5.93; N, 2.63 %. IR (nujol null, KBr): 3478(s), 3375(s), 3272(m), 2942(w), 2898(w), 1603(s), 1446(s), 1422(m), 1355(w), 1052(w), 1033(w), 692(s), 629(m), 559(m). MS (ESI): $^m/_z$ 872 {2x [$Cu_2(OAc)_4$(OAc)][Et_3NH].CH_3CN} – 2CH_3CN – 3OAc.

Electrochemistry

Electrochemistry was performed in a gas-tighten three-electrode system in which a vitreous carbon disk (Φ = 1 mm) was used as a working electrode, a carbon strip as counter electrode, and Ag / AgCl (inner reference solution: 0.45 mol L^{-1} [N*t*Bu_4]BF_4 + 0.05 mol L^{-1} [N*t*Bu_4]Cl in dichloromethane) against which the potential of ferrocenium / ferrocene couple is 0.55 V in 0.5 mol L^{-1} [N*t*Bu_4]BF_4 in CH_3CN. Ferrocene was added as an internal standard, and all potentials are quoted against ferrocenium / ferrocene couple (Fc^+ / Fc).

Procedure for ROP of ε-caprolactone

Typical polymerization procedures in the presence of one equivalent of benzyl alcohol (Table 1) are as follows. A toluene solution of **2** (0.04 mmol) and benzyl alcohol (0.04 mmol) were added into a Schlenk tube in the glove box at room temperature. The solution was stirred for 2 min., and then ε-caprolactone (10.0 mmol) along with 2 ml toluene was added to the solution. The reaction mixture was then palced into an oil bath pre-heated to the required temperature, and the solution was stirred for the prescribed time. The polymerization mixture was then quenched by the addition of excess glacial acetic acid (0.2 ml) and the resultant solution then poured into methanol (200 ml). The resultant polymer was then dried on filter paper was was dried *in-vacuo.*

Procedure for oxidation of benzene

Benzene (0.9 mL, 10 mmol), acetonitrile (2.5 mL) and catalytic amount of the copper complex (0.02 mmol) were placed into a reaction vessel equipped with cooling condenser and placed in an oil-bath. The reaction was heated at appropriate temperature for a period of time. When the reaction reached the specified temperature, appropriate amount of aqueous H_2O_2 (1.5 mL, 30 wt%) was slowly and carefully added in one-go. When the reaction was stopped and cooled, the volume of the reaction mixture was calibrated to 10 mL with CH_3CN in which there was an appropriate amount of toluene as an internal standard. To the calibrated reaction solution was added $MgSO_4$ (3 g) to remove the water in the reaction before being analyzed by gas chromatography. Quantitative analysis of both benzene and phenol was achieved by establishing their calibration curves with two linear equations under optimized conditions, $A_b = 0.0053\ W_b + 0.1266$ (R = 0.9986) and $A_p = 0.0034\ W_p - 0.1635$ (R = 0.9943) for benzene and phenol, respectively (Figs. S7 and S8, ESI), where A is the ratio of the peak areas of the analyte (benzene or phenol) and the internal standard toluene, W (mg) is the mass of the analytes, and the subscripts b and p denote benzene and phenol, respectively. The yield of phenol and benzene conversion was calculated as follows: phenol (mmol) / benzene initially used (mmol) ×100% and benzene–reacted (mmol) / benzene initially used (mmol) ×100%, respectively.

Crystallography details

Data collection

*For **1a**:* Single crystal X-ray diffraction data were collected using a Bruker SMART 1K CCD diffractometer using ω scans with narrow frames. Crystals were mounted at the end of a glass fibre under and held at 160 K in an Oxford Cryosystems nitrogen gas Cryostream.

*All other samples (except **3**):* Single crystal X-ray diffraction data were collected at room temperature (293 K) using an Agilent Technologies Xcalibur diffractometer operating with Mo Kαradiation and an Eos CCD detector in a series of *ω*-scans. [20] Data were integrated using standard procedure using CrysAlisProsoftware (Agilent). Data were corrected for absorption effects using a multi-scan method based on equivalents. In the case of **2f**, the crystals appeared to be unstable in the X-ray beam, presumably due to solvent loss. Given this, data for **2f** were collected at 150 K, in contrast to the other structures and were coated in a thin film of perfluoropolyether oil. Furthermore, the structure of **2f** at room temperature appears different to that at 150 K. At room temperature, the structure is

triclinic and centrosymmetric with a single copper cluster in the asymmetric unit. Upon cooling below about 240 K, a larger monoclinic cell of approximately twice the volume emerges. This low temperature form is non-centric and has two unique oxo clusters in the asymmetric unit.

For **3**: Data were collected on a Bruker SMART 1K CCD diffractometer at Daresbury SRS station 9.8 (λ = 0.6710 Å}. [21]

Structure solution and refinement

Structures were solved using automated direct methods within SHELXS-86 or intrinsic phasing within SHELXT. Structures were refined by full-matrix least squares refinement within SHELXL-2014 using all unique data. Hydrogen atoms were placed using a riding model. Where data were sufficiently good, methyl group orientations were refined. Many of the structures displayed disorder in the position of methyl groups or in solvent of crystallization. This disorder was modelled using standard techniques. In the case of structure **2e** it was not possible to locate the solvent molecules precisely and electron density in these regions was modelled using the Platon SQUEEZE routine. [22] For **2d** there was some evidence that the true lattice symmetry was primitive rather than C-centred, but it was not possible to obtain stable refinements with a primitive cell. The refinement in *C*2/*c*, which converged with R_F = 0.0734 and $wR(F^2)$ = 0.1317 (all data), was therefore retained.

CCDC 1040530 – 1040539 contain the supplementary crystallographic data for this paper.

Acknowledgements

Sichuan Normal University and the National Natural Science Foundation of China (grants 51443004 and 51273133) are thanked for financial support. The CCLRC is thanked for the award of beam-time at SRS Daresbury Laboratory (Station 9.8), and Dr. Simon J. Teat is thanked for scientific support.

Notes and references

[a] College of Chemistry and Materials Science, *Sichuan Normal University, Chengdu, 610066, China.*

[b] *Chemistry Department, Loughborough University, Loughborough, Leicestershire, LE11 3TU, U.K.*

[c] *Department of Chemistry, The University of Hull, Cottingham Rd, Hull, HU6 7RX, U.K.* Email: C.Redshaw@hull.ac.uk

[d] *College of Biological, Chemical Sciences and Engineering, Jiaxing University, Jiaxing 314001, China.*

[e] *EaStCHEM School of Chemistry, University of Edinburgh, David Brewster Road, Edinburgh, EH9 3FJ, Scotland.*

† Electronic Supplementary Information (ESI) available: [details of any supplementary information available should be included here]. See DOI: 10.1039/b000000x/

[1] I. Bratko and M. Gómez, *Dalton Trans*. 2013, **42**, 10664 and references therein.

[2] C.K. Williams, N.R. Brooks, M.A. Hillmyer and W.B. Tolman, *Chem. Commun*. 2002, 2132.

[3] A. Arbaoui, C. Redshaw, N.M. Sanchez-Ballester, M.R.J. Elsegood and D.L. Hughes, *Inorg. Chimica Acta* 2011, **365**, 96.

[4] L. Wang, W.-H. Sun, L. Han, Z. Li, Y. Hu, C. He and C. Yan, *J. Organomet. Chem.* 2002, **650**, 59.

[5] C.-Y. Tsai, B.-H. Huang, M.-W. Hsiao, C.-C. Lin and B.-T. Ko, *Inorg. Chem*. 2014, **53**, 5109.

[6] (a) S. Teipel, K. Griesar, W. Haase and B. Krebs, *Inorg. Chem.*1994,**33**, 456. (b) J. Reim, K. Griesar, W. Haase and B. Krebs, *J. Chem. Soc. Dalton Trans.* 1995, 2649.

[7] S. Mukherjee, T. Weyhermüller, E. Bothe, K. Wieghardt and P. Chaudhuri, *Eur. J. Inorg. Chem*. 2003, 863.

[8] P. Roy and M. Manassero, *Dalton Trans*. 2010, **39**, 1539.

[9] T. Ghosh, J. Adhikary, P. Chakraborty, P.K. Sukul, M. Sekhar Jana, T. K. Mondal, E. Zangrando and D. Das, *Dalton Trans.* 2014, **43**, 841.

[10] A. Kumar, R. Pandey, R.K. Gupta, M. Dubey and D.S. Pandey, *Dalton Trans*. 2014, **43**, 13169.

[11] J. T Guy Jr., J.C. Cooper, R.D. Gilardi and J.L. Flippen-Anderson, *Inorg Chem.* 1988, **27**, 635. (b) A.R. Paital, P.K. Nanda, S. Das, G. Aromi and D. Ray, *Inorg Chem.* 2006, **45**, 505.

[12] F.-F. Jian, P.-S. Zhao, H.-X. Wang and L.D. Wu, Bull. *Korean Chem. Soc.* 2004, **25**, 673.

[13] (a) P. Mukherjee, M.G.B. Drew and A. Figuerola, *Polyhedron* 2008, **27**, 3343. (b) H Karabiyuk, O. Erdem and M.Aygun, *J. Inorg. Organomet. Polym.* 2010, **20**, 142. (c) L. Mouni, M. Akkurt and S.O. Yildirm, *J. Chem. Crystallogr*. 2010, **40**, 169. (d) A. Kumar, M. Dubey, R.Pandey, R.K. Gupta, A. Kumar, A.C. Kalita and D. S. Pandey, *Inorg. Chem*. 2014, **53**, 4944. *The values in square brackets are for a system exhibiting significant tautomerism. [13b]

[14] (a) N.A. Bailey, D.E. Fenton, J. Lay, P.B. Roberts, J.-M. Latour and D. Limosin, *J. Chem., Soc. Dalton Trans*. 1986, 2681. (b) N.E. Borisova, M.D. Reshetova, T.V. Magdesieva, V.N. Khrustalev, G.G. Aleksandrov, M. Kuznetsov, R.S. Skazov, A.V. Dolganov, V.N. Ikorskiy, V.M. Novotortsev, I.L. Eremenko, I.I. Moiseev and Y.A. Ustynyuk, *Inorg. Chimica Acta* 2008, **361**, 2032. (c) M.-F. Zaltariov, M. Alexandru, M. Cazacu, S. Shova, G. Novitchi, C. Train, A. Dobrov, M.V. Kirillova, E.C.B.A. Alegria, A.J.L. Pombeiro and V.B. Arion, *Eur. J. Inorg. Chem*. 2014, 4946. (d) M. Pait, M. Shatruk, J. Lengyel, S. Gómez-Coca, A. Bauzá, A. Frontera, V. Bertolasi and D. Ray, *Dalton Trans*. 2015, in-press. Doi: 10.1039/C5DT90077H.

[15] L. Han, Y. Cui, Y. Li, W.-H. Sun, J. Du and J. Li, *J. Chem. Res*. 2003, 157.

[16] (a) V. McKee and S.S. Tandon, *J. Chem. Soc., Dalton Trans*. 1991, 221. (b) W.-X. Zhang, C.-Q. Ma, X.-N.Wang, Z.-G. Yu, Q.-J. Lin and D. –H. Jiang, *Chin. J. Chem*. 1995, **13**, 497. (c) R. Shakya, P.H. Keyes, M.J. Heeg, A. Moussawel, P.A. Heiney and C.N. Verani, *Inorg. Chem*. 2006, **45**, 7587. (d) R. Shakya, S.S. Hindo, L. Wu, S. Ni, M. Allard, M.J. Heeg,S.R.P. da Rocha, G.T. Yee, H.P. Hratchian and C.N. Verani, *Chem. Eur. J*. 2007, **13**, 9948. (e) S.S. Hindo, R. Shakya,R. Shanmugam, M.J. Heeg and C.N. Verani, *Eur. J. Inorg. Chem*. 2009, 4686. (f) P. Roy, M. Nandi, M. Manassero, M. Ricco, M. Mazzani, A. Bhaumik and P.Banerjee, *Dalton Trans*. 2009, 9543. (g) M.Sarkar, R.

Clerac, C. Mathoniere, N.G.R. Hearns, V. Bertolasi and D. Ray, *Inorg. Chem*. 2010, **49**, 6575. (h) M. Sarkar, R. Clerac, C. Mathoniere, N.G.R. Hearns, V. Bertolasi and D. Ray, *Inorg. Chem*. 2011, **50**, 3922. (i) D. Das, A. Guha, S. Das, P. Chakraborty, T.K. Mondal, S. Goswami and E. Zangrando, *Inorg. Chem. Commun*. 2012, **23**, 113. (j) M.S.Jana, S. Dey, J.L. Priego, R. Jimemez-Aparicio, *Polyhedron* 2013, **59**, 101. (k) A.K. Ghosh and D. Ray, *Polyhedron* 2013, **52**, 370. (l) S. Halder, S. Dey, C. Rizzoli and P. Roy, *Polyhedron* 2014, **78**, 85. (m) S. Das, L. Sorace, A. Guha, R. Sanyal, H. Kara, A. Caneschi, E. Zangrando and D. Das, *Eur. J. Inorg. Chem*. 2014, 2753. (n) M. Pait, E. Colacio and D. Ray, *Polyhedron* 2015, **88**, 90.

[17] (a) M. Labet and W. Thielemans, *Chem. Soc. Rev*. 2009, **38**, 3484. (b) A. Arbaoui and C. Redshaw, *Polym. Chem*. 2010, **1**, 801. (c) X. Rong and C. Chunxia, *Prog. Chem*. 2012, **24**, 1519.

[18] N. Ikpo, C. Hoffmann, L.N. Dawe and F.M. Kerton, *Dalton Trans*. 2012, **41**, 6631.

[19] (a) B. Xu, W. Zhong, Z. Wei, H. Wang, J. Liu, L. Wu, Y. Feng and X. Liu**,** *Dalton Trans.*, 2014, **43**, 15337. (b) X. You, Z. Wei, H. Wang, D. Li, J. Liu, B. Xu and X. Liu, *RSC Adv.*, 2014, **4**, 61790. (c) L. Wu, W. Zhong, B. Xu, Z. Wei, X. Liu, *Dalton Trans.*, 2015, **44**, 8013.

[20] *CrysAlisPro Softwarefor CCD diffractometers*, Agilent Technologies,2012.

[21] SAINT and SMART software for CCD diffractometers, Bruker AXS Inc.,Madison, USA, 2000.

[22] A. L. Spek, *Acta Crystallogr. Sect. A. Fundam. Crystallogr*. 1990, **46**, C34.

Table 2: Crystal data for the monomeric complexes **1a**, **1b** and polymeric **3**.

Identification code	**1a**	**1b**	**3**
Empirical formula	$C_{66}H_{82}CuN_4O_2$	$C_{64}H_{76}Cl_2CuN_4O_2$	$C_{18}H_{34}Cu_2N_2O_{10}$
Formula weight	1026.89	1067.72	565.55
Temperature	160(2) K	293(2) K	293(2) K
Wavelength	0.71073 Å	0.71073 Å	0.71073 Å
Crystal system	Monoclinic	Monoclinic	Monoclinic
Space group	$P2_1/c$	$P2_1/c$	$P2_1/n$
Unit cell dimensions	a = 9.8597(6) Å α= 90°. b = 12.1852(8) Å β= 97.5566(13)°. c = 24.1112(16) Å γ = 90°.	a = 10.0099(2) Å α= 90°. b = 12.1157(2) Å β= 97.487(2)°. c = 24.5154(5) Å γ = 90°.	a = 12.2105(4) Å α= 90°. b = 11.5458(4) Å β= 101.407(3)°. c = 17.7582(5) Å γ = 90°.
Volume	2871.6(3) Å^3	2947.80(10) Å^3	2454.10(14) Å^3
Z	2	2	4
Density (calculated)	1.188 Mg/m^3	1.203 Mg/m^3	1.531 Mg/m^3
Absorption coefficient	0.427 mm^{-1}	0.506 mm^{-1}	1.785 mm^{-1}
F(000)	1102	1134	1176
Crystal size	0.64 × 0.05 × 0.02 mm^3	0.25 × 0.25 × 0.20 mm^3	0.25 × 0.20 × 0.15 mm^3
Theta range for data collection	1.704 to 25.998°.	2.862 to 28.938°.	2.931 to 28.942°.
Index ranges	$-11 \le h \le 12$, $-15 \le k \le 14$, $-29 \le l \le 28$	$-13 \le h \le 12$, $-15 \le k \le 13$, $-33 \le l \le 20$	$-12 \le h \le 15$, $-15 \le k \le 9$, $-21 \le l \le 24$
Reflections collected	16148	14090	11719
Independent reflections	5606 [R(int) = 0.0835]	6775 [R(int) = 0.0246]	5625 [R(int) = 0.0257]

Completeness (to 2θ = 25.242 °)	99.6 %	99.8 %	99.8 %
Absorption correction	Empirical	Semi-empirical from equivalents	Semi-empirical from equivalents
Max. and min. transmission	0.992 and 0.772	1.000 and 0.958	1.000 and 0.835
Refinement method	Full-matrix least-squares on F^2	Full-matrix least-squares on F^2	Full-matrix least-squares on F^2
Data / restraints / parameters	5606 / 0 / 340	6775 / 7 / 331	5625 / 1 / 301
Goodness-of-fit on F^2	1.000	1.024	1.038
Final R indices [$I>2\sigma(I)$]	$R1$ = 0.0528, $wR2$ = 0.1035	$R1$ = 0.0502, $wR2$ = 0.1125	$R1$ = 0.0359, $wR2$ = 0.0771
R indices (all data)	$R1$ = 0.1074, $wR2$ = 0.1247	$R1$ = 0.0801, $wR2$ = 0.1270	$R1$ = 0.0517, $wR2$ = 0.0853
Largest diff. peak and hole	0.465 and –0.581 e.Å^{-3}	0.348 and –0.306 e.Å^{-3}	0.374 and –0.499 e.Å^{-3}

Table 3: Crystal data for $Cu_4OL_2(OAc)_4$ complexes.

Identification code	**2a**	**2b**	**2c**	**2c·MeCN**
Empirical formula	$C_{66}H_{86}Cu_4N_4O_{15}$	$C_{76}H_{94}Cu_4N_5O_{11}$	$C_{70.67}H_{88}Cu_4N_4O_{14.33}$	$C_{72}H_{86}Cu_4N_8O_{11}$
Formula weight	1429.54	1507.72	1477.00	1493.64
Temperature	293(2) K	293(2) K	293(2) K	293(2) K
Wavelength	0.71073 Å	0.71073 Å	0.71073 Å	0.71073 Å
Crystal system	Monoclinic	Monoclinic	Triclinic	Monoclinic
Space group	$C2/c$	$P2_1/n$	$P\bar{1}$	$P2_1/c$
Unit cell dimensions	a = 24.5344(10) Å b = 13.0252(4) Å c = 22.7527(8) Å α =90° β = 104.984(4)° γ = 90°.	a = 20.028(11) Å b = 15.1113(5) Å c = 25.249(4) Å α = 90° β = 98.68(4)° γ = 90°	a = 14.1438(9) Å b = 14.8853(5) Å c = 20.3062(5) Å α = 82.021(2)° β = 88.299(3)° γ = 64.613(5)°	a = 23.6777(5) Å b = 12.2318(3) Å c = 27.2068(6) Å α = 90° β = 113.205(2)° γ = 90°
Volume	7023.7(5) Å^3	7554(5) Å^3	3822.8(3) Å^3	7242.2(3) Å^3
Z	4	4	2	4
Density (calculated)	1.352 Mg/m^3	1.326 Mg/m^3	1.284 Mg/m^3	1.370 Mg/m^3
Absorption coefficient	1.259 mm^{-1}	1.171 mm^{-1}	1.158 mm^{-1}	1.222 mm^{-1}

F(000)	2984	3156	1541.3	3112
Crystal size	0.25 × 0.20 × 0.20 mm^3	0.40 × 0.35 × 0.20 mm^3	0.35 × 0.25 × 0.25 mm^3	0.35 × 0.25 × 0.20 mm^3
Theta range for data collection	2.953 to 28.956°.	2.956 to 28.991°.	2.923 to 29.028°.	2.854 to 29.127°.
Index ranges	-19 ≤ h ≤ 33, -10 ≤ k ≤ 17, -30 ≤ l ≤ 30	-25 ≤ h ≤ 27, -19 ≤ k ≤ 8, -32 ≤ l ≤ 24	-18 ≤ h ≤ 19, -20 ≤ k ≤ 20, -27 ≤ l ≤ 26	-23 ≤ h ≤ 32, -15 ≤ k ≤ 16, -36 ≤ l ≤ 29
Reflections collected	16990	43429	33076	41758
Independent reflections	8067 [*R*(int) = 0.0270]	17557 [*R*(int) = 0.0311]	17406 [*R*(int) = 0.0463]	16766 [*R*(int) = 0.0283]
Completeness (to 2θ = 25.242 °)	99.9 %	99.8 %	99.8 %	99.6 %
Absorption correction	Semi-empirical from equivalents	Semi-empirical from equivalents	Semi-empirical from equivalents	Semi-empirical from equivalents
Max. and min. transmission	1.000 and 0.787	1.000 and 0.840	1.000 and 0.843	1.000 and 0.881
Refinement method	Full-matrix least-squares on F^2	Full-matrix least-squares on F^2	Full-matrix least-squares on F^2	Full-matrix least-squares on F^2
Data / restraints / parameters	8067 / 6 / 386	17557 / 4 / 859	17406 / 12 / 838	16766 / 10 / 880
Goodness-of-fit on F^2	1.022	1.033	1.072	1.037
Final *R* indices [$I>2\sigma(I)$]	*R*1 = 0.0547, *wR*2 = 0.1321	*R*1 = 0.0426, *wR*2 = 0.0935	*R*1 = 0.0736, *wR*2 = 0.1908	*R*1 = 0.0388, *wR*2 = 0.0837
R indices (all data)	*R*1 = 0.0898, *wR*2 = 0.1537	*R*1 = 0.0727, *wR*2 = 0.1075	*R*1 = 0.1248, *wR*2 = 0.2288	*R*1 = 0.0547, *wR*2 = 0.0914
Largest diff. peak and hole	0.849 and –0.658 $e.Å^{-3}$	0.468 and –0.381 $e.Å^{-3}$	1.099 and –0.605 $e.Å^{-3}$	0.728 and –0.463 $e.Å^{-3}$

…Table 3 (cont).

Identification code	**2d**	**2e**	**2f**
Empirical formula	$C_{178}H_{183}Cl_6Cu_{12}N_{17}O_{33}$	$C_{72}H_{88}Cl_2Cu_4N_4O_{11}$	$C_{350}H_{183}Cu_{16}N_{31}O_{44}$
Formula weight	4063.58	1510.52	6764.65
Temperature	293(2) K	293(2) K	150(2) K
Wavelength	0.71073 Å	0.71073 Å	0.71073 Å

Crystal system	Monoclinic	Monoclinic	Monoclinic
Space group	*C*2/*c*	*C*2/*c*	$P2_1$
Unit cell dimensions	*a* = 65.736(3) Å *b* = 13.0482(4) Å *c* = 22.1089(5) Å α = 90° β = 98.395(2)° γ = 90°	*a* = 28.827(2) Å *b* = 28.771(3) Å *c* = 22.942(2) Å α = 90°. β = 120.445(11)°. γ = 90°.	*a* = 14.2390(6) Å *b* = 51.092(2) Å *c* = 14.3358(5) Å α = 90° β = 118.806(3) γ = 90°
Volume	18760.4(11) $Å^3$	16405(3) $Å^3$	9138.7(7) $Å^3$
Z	4	8	1
Density (calculated)	1.439 Mg/m^3	1.223 Mg/m^3	1.229 Mg/m^3
Absorption coefficient	1.488 mm^{-1}	1.141 mm^{-1}	0.976 mm^{-1}
F(000)	8336	6288	3536
Crystal size	0.35 × 0.30 × 0.25 mm^3	0.20 × 0.15 × 0.15 mm^3	0.42 × 0.38 × 0.32 mm^3
Theta range for data collection	2.896 to 29.172°.	3.009 to 25.601°.	1.594 to 25.285°.
Index ranges	$-55 \le h \le 87$, $-16 \le k \le 16$, $-27 \le l \le 25$	$-35 \le h \le 34$, $-34 \le k \le 31$, $-27 \le l \le 24$	$-17 \le h \le 17$, $-58 \le k \le 61$, $-15 \le l \le 17$
Reflections collected	50651	35204	48175
Independent reflections	20415 [*R*(int) = 0.0369]	15360 [*R*(int) = 0.0497]	27844 [*R*(int) = 0.1154]
Completeness (to 2θ = 25.242 °)	98.7 % (25.242 °)	99.5 %	98.9 % (25.242 °)
Absorption correction	Semi-empirical from equivalents	Semi-empirical from equivalents	Empirical
Max. and min. transmission	1.000 and 0.628	1.000 and 0.404	1.000 and 0.721
Refinement method	Full-matrix least-squares on F^2	Full-matrix least-squares on F^2	Full-matrix least-squares on F^2
Data / restraints / parameters	20415 / 27 / 1126	15360 / 0 / 838	27844 / 36 / 1980
Goodness-of-fit on F^2	1.050	1.038	0.874
Final *R* indices [$I>2\sigma(I)$]	*R*1 = 0.0497, *wR*2 = 0.1175	*R*1 = 0.0643, *wR*2 = 0.1577	*R*1 = 0.0777, *wR*2 = 0.1991
R indices (all data)	*R*1 = 0.0734, *wR*2 = 0.1317	*R*1 = 0.1204, *wR*2 = 0.1951	*R*1 = 0.1362, *wR*2 = 0.2448

Largest diff. peak and hole	0.918 and -0.632 e.Å^{-3}	0.681 and -0.580 e.Å^{-3}	0.611 and -1.187e.Å^{-3}